

## Effective Measures on Safety, Security, Hygiene and Disaster Prevention in Laboratories

T. Iimoto<sup>1</sup>, S. Hashima<sup>1</sup>, S. Mase<sup>1</sup>, D. Kaminushi<sup>1</sup>, K. Takamiya<sup>2</sup>

<sup>1</sup> *The University of Tokyo*

<sup>2</sup> *Integrated Radiation and Nuclear Science, Kyoto University*

**INTRODUCTION:** Important aspects of the study can be found in the following keywords, such as safety, security, hygiene and disaster prevention. Nuclear research reactor is one of representative target facilities of this study with these keywords under their operation. In addition, development of human resource and public literacy on nuclear science and technology is also within the scope of the re-search.

**RESEARCH APPROACH:** General research approach of this study is as follows. - It would not be a single year research, but maybe two to three years research for one theme. - Information source of facilities would not be only KUR, KUCA or the other facilities in Kyoto University, but also the Kindai university research nuclear reactor or the facility of National Institute of Fusion Science, etc. This research is an active joint-research with these relating facilities and positive researchers on safety management. Concrete discussion target in FY of 2023 was determined as ‘developing a set of educational videos for radiation protection in English for International Nuclear Science and Technology Academy (INSTA)’.

**WHAT IS INSTA?:** INSTA was established in the Asia and the Pacific region with strong support from the International Atomic Energy Agency (IAEA) through the Technical Cooperation Project aimed at supporting nuclear science and technology (NST) education at tertiary levels. INSTA's vision is to foster empowered regional NST educators. The key objectives are: (1) Facilitating linkages among academic institutions and stakeholders to optimize resources and advance NST education, (2) Fostering educational programs and platforms to address current and emerging needs in NST education, and (3) Envisioning and organizing activities to engage and motivate NST educators and stakeholders.

**CONCEPT AND CONTENTS OF RP-EDU-VIDEO:** To support the INSTA activity, the authors developed an English educational video entitled as ‘Radiation and Realism’, whose contents of the video are; <Part I> Human perception -Defining perception -Factors that influence perception such as past historical benefit vs risk -their importance in many areas such as decision making etc., <Part II> Exploring what is Myth? -Sharing the common Myths related to radiation -Participants can share their own perception & discuss - some educators from non- NST background may also have similar perception. -May even share the stigma post Goiania incidents, can also include case studies of other incidents, <Part III> Radiation in reality -Elements and actual conditions of exposure in nature -Generals of Human Effects -Epidemiology of A-bomb and India -ICRP History and Principles of Radiation Protection -Justification, Optimization & Dose constraints -Radiation Application.

# Application of KURAMA-II to Radiation Monitoring of Forests in Fukushima Prefecture

A. Maekawa, K. Kusakabe and M. Tanigaki<sup>1</sup>

*Fukushima Prefectural Centre for Environmental Creation*  
<sup>1</sup>*Institute for Integrated Radiation and Nuclear Science, Kyoto University*

**INTRODUCTION:** KURAMA (Kyoto University RAdiation MApping system)-II is a radiation measurement system characterized by its compactness, autonomous operation, and acquisition of pulse-height spectrum data (Fig. 1) [1]. KURAMA-II measures ambient dose equivalent rate (hereafter called air dose rate) and GPS position and automatically transmits them to a dedicated cloud server. In this study, we evaluated the effectiveness of a backpack-style KURAMA-II (Fig. 2) for the radiation monitoring of forests in Fukushima prefecture by comparing it with a NaI(Tl) scintillation survey meter conventionally used in radiation monitoring.

**EXPERIMENTS:** A 10 m interval grid (30 x 50 m) was established in five forests. The air dose rates were measured by a KURAMA-II in a backpack with a CsI (TI) scintillation detector (C12137-01, Hamamatsu Photonics) walking along the grid line. The air dose rate and GPS position were measured every second. The air dose rate at 1 m above the center point of each grid was also measured by a NaI (TI) scintillation survey meter (TCS-172B, Aloka). All measurement was carried out in Dec. 2023 - Jan. 2024.

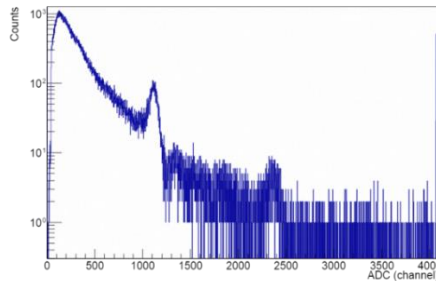


Fig. 1. A typical example of pulse-height spectrum obtained by KURAMA-II measurement.



Fig. 2. KURAMA-II in a backpack.

**RESULTS:** Table 1 shows the air dose rate range at each forest site. All the measurement result of a survey meter were within the range of KURAMA-II. A typical radiation map by KURAMA-II and a survey meter is shown in Fig. 3 (site D). The spatial distribution of air dose rate measured by KURAMA-II was well consistent with that of a survey meter. In the present study, KURAMA-II showed promising performance in revealing a more detailed distribution of air dose rates.

Table 1. The air dose rate range at each forest site.

Site	Air dose rate by KURAMA-II (μSv/h)	Air dose rate by survey meter (μSv/h)
A	0.08-0.18	0.11-0.15
B	0.11-0.26	0.21-0.23
C	0.13-0.25	0.17-0.20
D	0.03-0.12	0.07-0.11
E	0.27-0.71	0.44-0.59

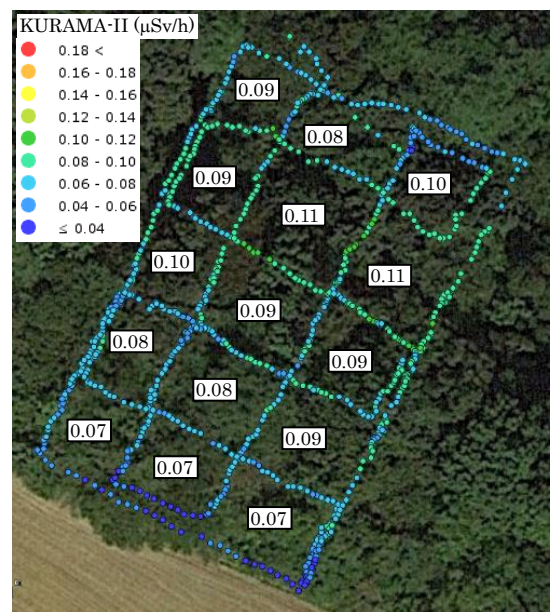


Fig. 3. The radiation map created by KURAMA-II (colored dots) and a survey meter (numerical data).

**REFERENCES:**

[1] M. Tanigaki *et al.*, Nucl. Instrum. Meth. Phys. Res., **781** (2015) 57-64.

## Nationwide Survey of Chlorine and Bromine Concentration in Dewatered Sewage Sludge Measured by Neutron Activation Analysis

T. Matsunaga<sup>1</sup>, R. Homma<sup>1</sup>, S. Fukutani<sup>2</sup>, K. Oshita<sup>1</sup>, and M. Takaoka<sup>1</sup>

<sup>1</sup>Department of Environmental Engineering, Graduate School of Engineering, Kyoto University

<sup>2</sup>Research Reactor Institute, Kyoto University (KURRI)

**INTRODUCTION:** In recent years, the use of sewage sludge as fertilizer has been promoted, but sewage sludge contains not only beneficial components but also harmful ones. In this study, neutron activation analysis (NAA) was performed on dewatered sewage sludges sampled from 34 wastewater treatment plants across Japan to analyze chlorine and bromine concentrations.

**EXPERIMENTS:** The dewatered sewage sludges were collected from 34 wastewater treatment plants in Japan in 2023, dried at 105°C, and then homogenized with a crusher. NAA was performed four times for each sample. Samples were irradiated for 1-5 min with a thermal neutron flux of  $2.0\text{-}2.4 \times 10^{13} \text{ cm}^{-2} \cdot \text{sec}^{-1}$  at KURRI.  $^{38}\text{Cl}$  ( $t^{1/2} = 37.18 \text{ min}$ ,  $E_{\gamma} = 1642, 2168 \text{ keV}$ ) and  $^{80}\text{Br}$  ( $t^{1/2} = 17.68 \text{ min}$ ,  $E_{\gamma} = 616, 666 \text{ keV}$ ) were measured by using a Ge semiconductor detector for 300 sec.

**RESULTS:** Fig.1 shows histograms and cumulative relative frequency graphs of chlorine and bromine concentrations. For chlorine concentration, most of the sludge samples were in the low concentration range under 2,500 mg/kg-Dry-Solid(DS), while there were a few samples with extremely high concentrations. Also, half of the sludge samples had bromine concentrations in the relatively low range of 20-40 mg/kg-DS, while there were some samples with high concentrations. The treatment plant with the highest chlorine concentration had a large amount of industrial wastewater originating from chemical plants flowing into it, which could be affected by the industrial products contained in this wastewater.

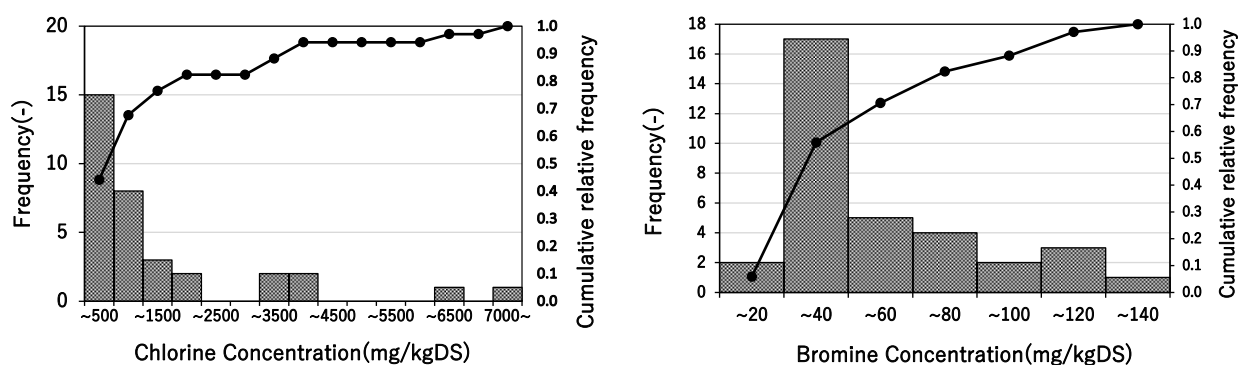


Fig.1. Histograms and cumulative relative frequency graphs of chlorine and bromine concentrations

The results were compared with those of chlorine and bromine concentrations from neutron activation analysis of dewatered sludge from 32 sewage treatment plants nationwide sampled between 2015 and 2016 by Chen *et al.* [1]. Statistical analysis of the Wilcoxon rank sum test showed that no significant difference existed between the results by Chen *et al.* for bromine concentration (p-value 0.7435), but a significant difference existed for chlorine concentration (p-value 0.0044). It is suggested that this is because the dewatered sludge sampled in this study included several samples that were thought to be inflow of industrial wastewater. Also, due to the difference in age between 2015 and 2023, the possibility exists that industrial development has increased the production of industrial products, resulting in an increase in chlorine emissions.

### REFERENCES:

[1] M. Chen *et al.*, Science of the Total Environment, **752** (2021) 141857.

## Study for activity measurement of $^{41}\text{Ar}$ and $^{133}\text{Xe}$ using a plastic scintillator and an calibrated ionization chamber

Takahiro Yamada<sup>1,2</sup>, Yuya Soeta<sup>2</sup>, Seiya Ohtsuka<sup>2</sup>, Ren Ichikawa<sup>2</sup>, Rio Furukawa<sup>3</sup> and Hiroshi Yashima<sup>4</sup>

<sup>1</sup>Atomic Energy Research Institute, Kindai University

<sup>2</sup>Graduate school of Science and Engineering, Kindai University

<sup>3</sup>National Metrology Institute of Japan

<sup>4</sup>Institute for Integrated Radiation and Nuclear Science, Kyoto University

**INTRODUCTION:** To calibrate monitors used for measuring radioactive noble gases in nuclear facilities, use of activity reference measurement standard gases shall be required. The authors have been conducting absolute measurements of activity using a  $4\pi\beta\text{-}\gamma$  coincidence spectroscopy with plastic scintillator detectors, targeting  $^{41}\text{Ar}$  and  $^{133}\text{Xe}$  generated at KUR-SLY since FY2021, aiming to establish standards [1]. In this year, activity measurement using an inner-through-type ionization chamber, denoted later as IC, was conducted to compare with the result obtained by  $4\pi\beta\text{-}\gamma$  coincidence spectroscopy.

**EXPERIMENTS:** A 5 ml acrylic container was filled with pure argon gas to produce  $^{41}\text{Ar}$  via  $^{40}\text{Ar}(n, \gamma)^{41}\text{Ar}$  reaction. As for  $^{133}\text{Xe}$  naturally occurring xenon gas consists of seven stable isotopes was filled into the 60 ml acryl container to produce  $^{133}\text{Xe}$  via  $^{132}\text{Xe}(n, \gamma)^{133}\text{Xe}$  reaction. Each gas container was irradiated for 60 s at the bottom of KUR-SLY operating at 1 MW thermal output.

An acrylic gas container was used as the  $\beta$ -detection part of the measurement system. The entire inner wall of the container was covered with a 1 mm thick plastic scintillator (PS), with a content volume of 80 ml. A photomultiplier tube (PMT) was connected to the top of the container and stored in a light-shielded case. The  $\beta$ -detector was placed onto the Ge detector, and the signal outputs from the  $\beta$ - and  $\gamma$ -detectors were fed to the signal inputs of a list-mode multi-channel analyzer (MCA). The 1.5L IC (Model I-409601, Ohkura Electric Co., Ltd.) was used to measure the activity of  $^{41}\text{Ar}$  and  $^{133}\text{Xe}$ . The calibration factor [pA per Bq cm<sup>-3</sup>] required to convert the output current from the IC to the concentration of radioactive gases, was previously evaluated to be 0.288 pA Bq<sup>-1</sup> cm<sup>3</sup> for  $^{41}\text{Ar}$  [1]. For  $^{133}\text{Xe}$ , since the calibration factor has not been evaluated, we attempted to identify the nuclide by observing the decrease of the currents comparing the half-life.

**RESULTS:** In the measurement of diluted  $^{41}\text{Ar}$  using IC, activity concentration was determined as 21.8 Bq cm<sup>-3</sup> at around 9 hours after irradiation. A half-life of 108.9 min was obtained from a set of IC measurements, shorter than the recommended half-life of  $109.611 \pm 0.038$  min [2]. The  $\beta$ -counting efficiency, determined as  $n_c/n_\gamma$  in the coincidence count measurement, was 0.920. Preliminary results of activity concentration determined from the  $4\pi\beta\text{-}\gamma$  coincidence spectroscopy was 22.7 Bq cm<sup>-3</sup>. Fig. 1 shows changes in the output currents of the IC for Xe gas. The apparent half-lives of Xe gas were evaluated to be 3.5 d and 5.5 d from 48 to 84 hours and 96 to 126 hours after irradiation, respectively. The present difference could be due to the fact that the impurity nuclides, which have a shorter half-life than  $^{133}\text{Xe}$ , decayed over time, resulting in a higher relatively higher activity of  $^{133}\text{Xe}$  compared to that of the impurity nuclides. Further study should be required to determine activity of Xe gases.

### REFERENCES:

- [1] A. Yunoki *et al.*, Annl. Rep. of Coop. Res. at Kindai Univ. Reactor (2020) (in Japanese).  
 [2] Bé, M., 2011. Table of Radionuclides.

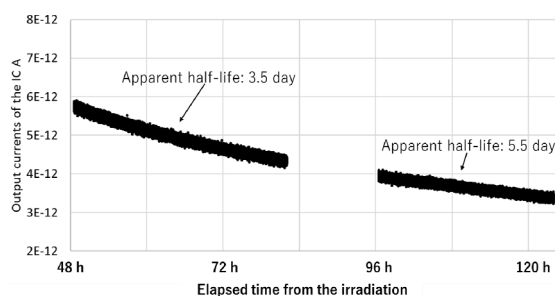


Fig. 1. The IC output currents in a series of Xe gas measurement.



## Determination of chlorine content in the cable jackets of power supplies in accelerator facilities

G. Yoshida, K. Nishikawa<sup>1</sup>, E. Watanabe, K. Tsugane, K. Takahashi, T. Bui<sup>2</sup>, and H. Yashima<sup>3</sup>,

*Radiation Science Center, KEK*

<sup>1</sup>*Department of Safety Management, QST*

<sup>2</sup>*Accelerator Science Program, SOKENDAI*

<sup>3</sup>*Institute for Integrated Radiation and Nuclear Science, Kyoto University*

**INTRODUCTION:** A large-scale accelerator facility, such as the 12 GeV proton synchrotron facility of KEK (KEK-PS), produces various radionuclides. Some of these nuclides remain for long periods and become apparent as a radioactive waste when its decommissioning work. Although power cables are used in accelerator facilities in smaller quantities than concrete or metals (magnets and coils), the cable jacket is made from chlorine-containing plastic. It produces  $^{36}\text{Cl}$ , which has a long half-life of 300,000 years for pure  $\beta$ -nucleus (difficult to measure), through the  $(n,\gamma)$  reaction of  $^{35}\text{Cl}$ . We are developing the determination method for  $^{36}\text{Cl}$  activity in cable jackets by Accelerator Mass-Spectrometry (AMS). Still, we are faced with the problem of the chlorine content in the jackets being unknown in many cases. Neutron activation analysis has been used to analyze chlorine in various samples and could be established to determine the chlorine contents of cable jackets.

**EXPERIMENTS:** The power cable jacket of the septum magnet of KEK-PS was collected, cut into 1-5 mm pieces, washed with water and ethanol, and weighed 100 mg to prepare irradiation samples. The chlorine-containing plastic standards (JSM\_P713-1 series) distributed by the JFE Techno-Research Co. were employed as references and prepared in the same way. Samples were irradiated at Pn-3 with 1 MW for 10 s, and  $\gamma$ -ray spectrometry of  $^{38}\text{Cl}$  was conducted with a Ge detector immediately after irradiation.

**RESULTS:** The  $\gamma$ -ray spectra of the representative sample and standard are shown in Fig. 1. The  $\gamma$ -ray peaks attributed to  $^{38}\text{Cl}$  were observed in both standards and the cable jacket samples. From the measurement result of five different chlorine contents of standards, we found a good correlation between the 1634 keV  $\gamma$ -ray count rates and chlorine contents. Based on the calibration curve prepared from the standard samples, the chlorine content of the cable jacket was estimated to be approximately 17%.

In conclusion, it was found that chlorine content in power cable jackets can be determined accurately using Neutron activation analysis.

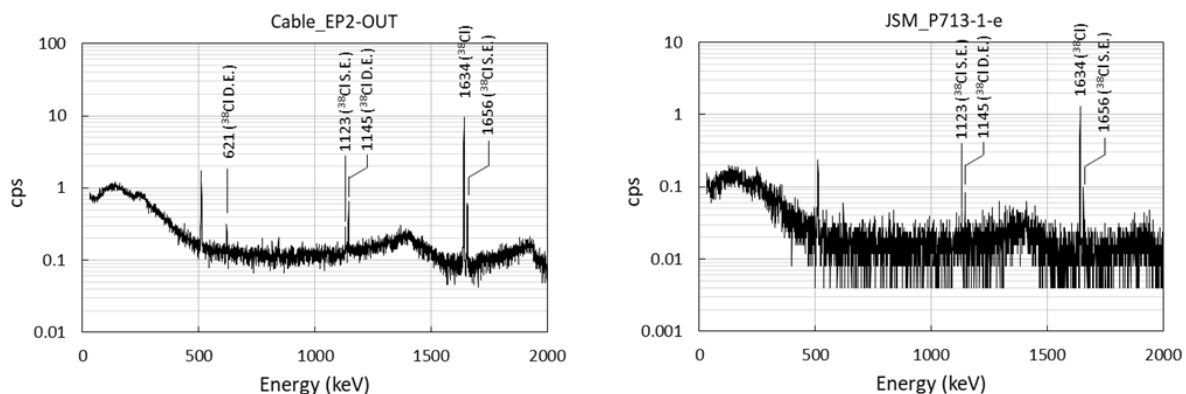


Fig. 1.  $\gamma$ -ray spectra of representative cable jacket sample (right) and standard (left)

## Measurement of Number-Based and Radioactivity-Based Size Distributions of Aerosol Particles Generated in the Accelerator Room of an Electron LINAC Facility Using Screen-Type Diffusion Battery

Y. Oki, K. Takamiya and M. Inagaki

*Institute for Integrated Radiation and Nuclear Science, Kyoto University*

**INTRODUCTION:** With recent advances in high-intensity and high-energy accelerators, ensuring accelerator radiation safety has become increasingly important. We have previously reported on the use of a screen-type diffusion battery (SDB) technique to measure the particle size distribution of radioactive aerosols generated in accelerator rooms, which is useful for internal exposure assessment. This report describes the results of two methods of particle size measurement using SDB and the current problems.

**EXPERIMENTS:** When fine aerosol particles of about 100 nm or less pass through a stack of wire screens, some of the particles are deposited on the wire surface of the screen by diffusion, depending on the particle size. The percentage of particles that can pass through the screen (penetration ratio) is expressed as a function of particle size, roughness and number of screens, and particle flow rate. By measuring the penetration ratio by varying the number of screens or flow rate, the particle size can be calculated from the theoretical equation.

Radioactive aerosols produced by air irradiation using an irradiation chamber at the electron linac of our institute. The irradiated air containing the aerosols was introduced to the SDB consisting of multiple screens and a backup PTFE filter. This experiment was conducted in two ways. *Method 1:* Varying the flow rate: The irradiated air was simultaneously introduced to the SDB line and the compensation line. The SDB comprised two screens. The flow rate of air introduced into the SDB was varied from 0 to 15 L/min. At the same time, to keep the flow rate in the irradiation chamber constant, the flow rate into the compensation line was varied so that the total flow rate in the SDB line and the compensation line was constant. *Method 2:* Varying the number of screens: A maximum of 40 wire screens were used for the SDB. In addition, activity of the selected screens and the backup filter was simultaneously measured using a single large imaging plate [1]. The penetration ratio for the *i*-th screen was estimated from the intensity of photostimulated luminescence of the screens and the filter.

**RESULTS:** Since a stable lognormal-type particle size distribution was observed in the SMPS (scanning mobility particle sizer) measurement performed simultaneously with the SDB sampling, the geometric mean and geometric standard deviation of the particle diameter were calculated, assuming a lognormal particle size distribution, by fitting the penetration ratios obtained by each of the two methods to the theoretical equation [2]. Number-based particle diameter tended to increase with increasing beam current (20-100  $\mu$ A) in the SDB measurements, ranging from 20 to 60 nm. At the same beam conditions, the size distributions obtained with Methods 1 and 2 were in good agreement, and the results were also in very good agreement with the SMPS measurements. In the radioactivity-based size measurement for  $^{13}\text{N}$ -bearing aerosol particles, adsorptive gases such as  $\text{H}^{13}\text{NO}_3$  adsorbed on the filters and screens sometimes may cause errors in the fitting results. An effective compensation technique was discussed to eliminate the influence.

### REFERENCES:

- [1] Y. Oki *et al.*, J. Radiat. Prot. Res., **41** (2016) 216-221.
- [2] Y.S. Cheng and H.C. Yeh, J. Aerosol Sci., **11** (1980) 313-320.

## Application of KURAMA-II to the analysis of air dose rate distribution around monitoring posts

M. Hosoda<sup>1</sup>, M Watanabe<sup>1</sup>, H Tanaka<sup>1</sup>, M. Tanigaki<sup>2</sup>

<sup>1</sup>Japan Chemical Analysis Center

<sup>2</sup>Institute for Integrated Radiation and Nuclear Science, Kyoto University

**INTRODUCTION:** In the nationwide survey of environmental radioactivity levels commissioned by the Nuclear Regulation Authority, air dose rates are measured using portable monitoring posts at about 80 locations in Fukushima Prefecture. Air dose rates obtained by monitoring posts are representative values for each location, and we do not see the detailed distribution of the air dose rate due to the uneven distribution of the artificial radionuclide around the monitoring posts.

In this study, we measured air dose rates around the portable monitoring posts located in a difficult-to-return zone in Fukushima Prefecture by a car-borne survey system KURAMA (Kyoto University Radiation MAPPING system)-II as a walking survey. We analyzed the distribution of the air dose rate and the radioactive cesium using radiation mapping methods.

**EXPERIMENTS:** We walked with KURAMA-II around the monitoring post at the Ogaki Post Office in Namie Town, Fukushima Prefecture. The data were grouped by a 1 m mesh centered on the monitoring post, and an areal evaluation was performed by displaying the data on a map. From the measured air dose rate data and the pulse-height spectrum data of each mesh, the air dose rate from the natural radioisotopes and that given by the artificial radioisotopes, i.e., Cs-134 and Cs-137, were evaluated respectively using Equation (1) defined in ref. [1],

$$\begin{cases} \dot{D}_n = 0.062x \\ D_a = \dot{D}_t - \dot{D}_n, \end{cases} \quad (1)$$

where  $\dot{D}_t$  is the measured air dose rate ( $\mu\text{Sv/h}$ ),  $x$  is the counting rates from 1400 to 2000 keV obtained by spectrum data,  $\dot{D}_n$  is the air dose rate given by natural radioisotopes, and  $D_a$  is that given by the artificial radioisotopes.

**RESULTS:** Figure 1 shows the 1 m  $\times$  1 m mesh map of the air dose rate obtained by the present walking survey. The average air dose rate measured by the monitoring post was 2.12  $\mu\text{Gy/h}$ , whereas the average air dose rates per 1 m  $\times$  1 m mesh obtained by the walking survey ranged from 0.92 to 6.09  $\mu\text{Gy/h}$ . Figure 2 shows the spectrum data of the meshes (1), (2) and (3) in Figure 1, having different air dose rates. The counts below 1000 keV differed depending on the mesh, suggesting that the differences in the air dose rates are due to the uneven distribution of Cs-134 and Cs-137. Figure 3 shows the map display of the air dose rate given by natural radioisotopes for each mesh calculated by Equation (1). From these results, the differences in the air dose rates are not due to the uneven distribution of natural radioisotopes but the artificial radioisotopes, Cs-134 and Cs-137.

### REFERENCES:

[1] M. Ando *et al.*, T. J. At. Energy Soc. Jpn., **20(1)** (2021) 34-39. (In Japanese)

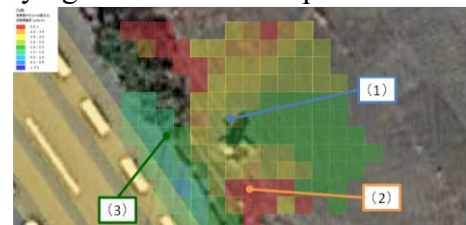


Figure 1. the 1 m  $\times$  1 m mesh map of the air dose rate ( $\mu\text{Gy/h}$ ) obtained by the present walking survey.

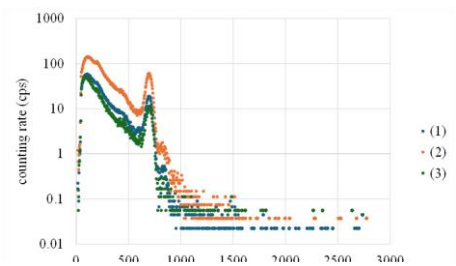


Figure 2. The spectrum data of mesh (1), (2), and (3) in Figure 1.



Figure 3. The map display of the air dose rate given by natural radioisotopes ( $\mu\text{Sv/h}$ ) for each mesh calculated by Equation (1).